Non-equilibrium gas flow and heat transfer in a bottom heated square microcavity

Giorgos TATSIOS [1], Manuel H. VARGAS[1], Stefan K. STEFANOV[2], Dimitris VALOUGEORGIS[1,*]

* Corresponding author: Tel.: ++30 24210 74058; Fax: ++30 24210 74085; Email: diva@uth.gr
1: Department of Mechanical Engineering, University of Thessaly, Greece
2: Institute of Mechanics, Bulgarian Academy of Sciences, Sofia, Bulgaria

Abstract The flow of a rarefied gas in a square enclosure with a bottom wall at high temperature and the other three walls at the same low temperature is investigated. The flow configuration is simulated both deterministically, using the non-linear Shakhov kinetic model and stochastically, using the DSMC method. Excellent agreement between the two approaches is obtained. The flow is characterized by the reference Knudsen number and the temperature ratio. It is found that along the side walls the velocity of the gas is not necessarily from cold-to-hot regions due to thermal creep, but from hot-to-cold as well. The effect of the flow parameters to this configuration, including the not well theoretically defined flow from hot-to-cold, is investigated and results are provided in the whole range of the Knudsen number for small, moderate and large temperature differences.
Keywords: Kinetic Theory, Rarefied Gas Dynamics, Thermal Creep, Knudsen Number, GASMEMS

1. Introduction

Rarefied flows in microcavities due to heated walls have received a lot of attention recently, due to their application in vacuum packed MEMS (Stone et al., 2004; Yang et al., 2005; Liu et al., 2007), micropumps (Sone et al., 1996; Alexeenko et al., 2006), microactuators and microsensors (Ketsdever et el., 2012; Vargas et al., 2012). They are also commonly applied in benchmarking of novel numerical schemes (Masters, Ye, 2007; Rana et al., 2012; Huang et al., 2013) and in the investigation of non-equilibrium phenomena that arise in such flows (Cai, 2008; Sone, 2009; Naris, Valougeorgis, 2006).

The main dimensionless parameter characterizing those flows is the Knudsen number, which is the ratio of the mean free path over a characteristic length of the flow. Flows characterized by small Knudsen numbers, that are in the slip or early transition regimes can be modeled by the conventional Navier-Stokes-Fourier (NSF) analysis with the appropriate slip and jump boundary conditions (Sone, 2002), or with higher order continuum models (Struchtrup, Taheri, 2011). At higher values of the Knudsen number, when the flow is in the transition and free molecular regimes the NSF approach fails and a kinetic approach must be applied.

In the present work both the non-linear Shakhov kinetic model and the DSMC method are used to solve this microcavity flow configuration in the whole range of the Knudsen number for various temperature differences between the high temperature of the heated wall and the low temperature of the other three walls.

2. Flow configuration

A monatomic rarefied gas is contained in a 2D enclosure with square cross section of side W. The cross section of the enclosure and the origin of the coordinate system are shown in Fig. 1. The bottom wall is at temperature T_H, while the other three walls are kept at a temperature T_C, with $T_C < T_H$. To avoid discontinuities at the two bottom corners, the temperature of the bottom plate close to the two corners (5% of the total length) is linearly decreased to match the side walls temperature.

Due to thermal creep a flow is expected near the side walls directed from cold-to-hot regions and to ensure mass conservation a

flow near the symmetry axis ($x'=0$) is expected in the opposite direction. This would create two counter rotating vortices in the enclosure. It turns out that in addition to these vortices, even at small Knudsen numbers, two more vortices appear in the upper part of the enclosure, with a flow along the lateral walls from hot-to-cold regions. All four vortices are shown in Fig. 1, with the former ones denoted by the I and the latter unexpected ones by II. The detailed flow pattern depends on the Knudsen number and the temperature ratio.

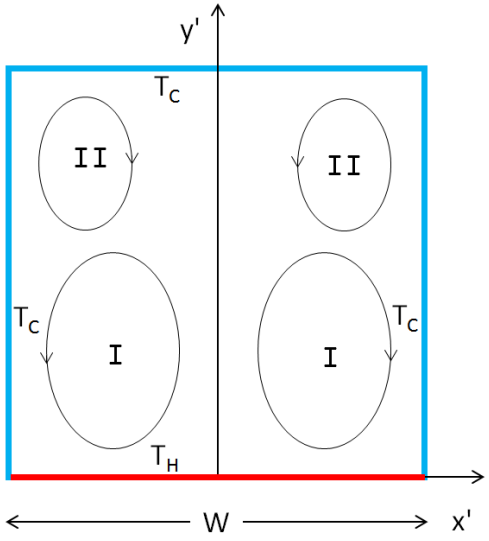

Fig. 1. View of the bottom heated square microcavity with the flow pattern of vortices I and II.

The 2D macroscopic quantities of interest are the number density N , the two component velocity vector $\boldsymbol{U}=\left[U_x,U_y\right]$, the shear stress tensor P_{xy} , the temperature distribution T and the two component heat flux vector $\boldsymbol{Q}=\left[Q_x,Q_y\right]$, while the gas pressure is given by the ideal gas law $P=Nk_BT$, with k_B denoting the Boltzmann constant.

The problem is characterized by the reference Knudsen number defined as

$$Kn_0=\frac{\sqrt{\pi}}{2}\frac{\mu_0\upsilon_0}{P_0W} \qquad (1)$$

and the temperature ratio T_C/T_H. In Eq. (1) P_0 is the reference pressure, W is the side length of the square cavity, μ_0 is the gas viscosity at reference temperature T_0 and $\upsilon_0=\sqrt{2k_BT_0/m}$ is the most probable molecular speed (m denotes the molecular mass). The reference number density N_0 is related to the reference pressure and temperature according to $P_0=N_0k_BT_0$. The following dimensionless quantities are introduced:

$$x=x'/W,\ \ y=y'/W,\ \ n=N/N_0$$
$$u_x=U_x/\upsilon_0,\ \ u_y=U_y/\upsilon_0,\ \ p=P/P_0 \qquad (2)$$
$$\tau=T/T_0,\ \ q_x=Q_x/\left(P_0\upsilon_0\right),\ \ q_y=Q_y/\left(P_0\upsilon_0\right)$$

The space variables are $x\in\left[-0.5,0.5\right]$ and $y\in\left[0,1\right]$, while n , $\left(u_x,u_y\right)$, p , τ , with $p=n\times\tau$ and $\left(q_x,q_y\right)$ are the distributions of the number density, the two components of the velocity vector, the gas pressure and temperature and the two components of the heat flux vector respectively. The Inverse Power Law (IPL) interaction (Naris, Valougeorgis, 2006) is applied yielding a viscosity of the form $\mu=\mu_0\tau^{\omega}$, with the parameter $\omega\in\left[1/2,1\right]$. The two limiting cases of $\omega=1/2$ and $\omega=1$ correspond to hard sphere and Maxwell molecules.

3. Deterministic and stochastic kinetic modeling

The problem is solved both in a deterministic and stochastic manner. The deterministic modeling is based on the direct solution of the nonlinear Shakhov kinetic model (Shakhov, 1968) and the stochastic modeling on the DSMC method (Bird, 1994). In both cases purely diffuse gas-surface interaction is considered.

3.1 Formulation of the kinetic model

The main unknown is the distribution function $f=f\left(x',y',\boldsymbol{\xi}\right)$, with $\boldsymbol{\xi}=\left(\xi_x,\xi_y,\xi_z\right)$ denoting the molecular velocity vector, which obeys the nonlinear Shakhov equation given by

$$\xi_x\frac{\partial f}{\partial x'}+\xi_y\frac{\partial f}{\partial y'}=\frac{P}{\mu}\left(f^S-f\right) \qquad (3)$$

where P is the local pressure and $\mu = \mu(T)$ is the viscosity at local temperature T. The Shakhov relaxation function f^S is given in (Shakhov, 1968; Sharipov, Seleznev, 1998).

Introducing the dimensionless quantities of Eq. (2) into Eq. (3) and following a well-known projection procedure to eliminate the $z-$component of the molecular velocity the following system of integro-differential equations is obtained:

$$\zeta_x \frac{\partial \varphi}{\partial x} + \zeta_y \frac{\partial \varphi}{\partial y} = \frac{1}{Kn_0} \frac{\sqrt{\pi}}{2} n\tau^{1-\omega} \left(\varphi^S - \varphi\right) \quad (4)$$

$$\zeta_x \frac{\partial \psi}{\partial x} + \zeta_y \frac{\partial \psi}{\partial y} = \frac{1}{Kn_0} \frac{\sqrt{\pi}}{2} n\tau^{1-\omega} \left(\psi^S - \psi\right) \quad (5)$$

Here, the main unknowns are the reduced distributions functions $\varphi = \varphi\left(x, y, \zeta_x, \zeta_y\right)$ and $\psi = \psi\left(x, y, \zeta_x, \zeta_y\right)$, with ζ_x and ζ_y denoting the dimensionless components on the molecular velocity vector, while

$$\varphi^S = \varphi^M \left(1 + \frac{4}{15} \frac{1}{n\tau^2} \left[q_x \left(\zeta_x - u_x\right) + q_y \left(\zeta_y - u_y\right)\right] \times \left[\left[\left(\zeta_x - u_x\right)^2 + \left(\zeta_y - u_y\right)^2\right] / \tau - 2\right]\right) \quad (6)$$

and

$$\psi^S = \psi^M \left(1 + \frac{4}{15} \frac{1}{n\tau^2} \left[q_x \left(\zeta_x - u_x\right) + q_y \left(\zeta_y - u_y\right)\right] \times \left[\left[\left(\zeta_x - u_x\right)^2 + \left(\zeta_y - u_y\right)^2\right] / \tau - 1\right]\right) \quad (7)$$

with the reduced local Maxwellians given by

$$\varphi^M = \frac{n}{\pi\tau} \exp\left[-\left[\left(\zeta_x - u_x\right)^2 + \left(\zeta_y - u_y\right)^2\right] / \tau\right] \quad (8)$$

$$\psi^M = \frac{n}{2\pi} \exp\left[-\left[\left(\zeta_x - u_x\right)^2 + \left(\zeta_y - u_y\right)^2\right] / \tau\right] \quad (9)$$

The macroscopic quantities can be expressed as moments of φ and ψ:

$$n(x, y) = \int_{-\infty}^{\infty} \int_{-\infty}^{\infty} \varphi d\zeta_x d\zeta_y \quad (10)$$

$$u_x(x, y) = \frac{1}{n} \int_{-\infty}^{\infty} \int_{-\infty}^{\infty} \zeta_x \varphi d\zeta_x d\zeta_y \quad (11)$$

$$u_y(x, y) = \frac{1}{n} \int_{-\infty}^{\infty} \int_{-\infty}^{\infty} \zeta_y \varphi d\zeta_x d\zeta_y \quad (12)$$

$$\tau(x, y) = \frac{2}{3n} \int_{-\infty}^{\infty} \int_{-\infty}^{\infty} \left[\left(\zeta_x^2 + \zeta_y^2\right)\varphi + \psi\right] d\zeta_x d\zeta_y - \frac{2}{3}\left(u_x^2 + u_y^2\right) \quad (13)$$

$$p_{xy}(x, y) = 2 \int_{-\infty}^{\infty} \int_{-\infty}^{\infty} \left(\zeta_x - u_x\right)\left(\zeta_y - u_y\right) \times \varphi d\zeta_x d\zeta_y \quad (14)$$

$$q_x(x, y) = \int_{-\infty}^{\infty} \int_{-\infty}^{\infty} \left[\left[\left(\zeta_x - u_x\right)^2 + \left(\zeta_y - u_y\right)^2\right]\varphi + \psi\right] \times \left(\zeta_x - u_x\right) d\zeta_x d\zeta_y \quad (15)$$

$$q_y(x, y) = \int_{-\infty}^{\infty} \int_{-\infty}^{\infty} \left[\left[\left(\zeta_x - u_x\right)^2 + \left(\zeta_y - u_y\right)^2\right]\varphi + \psi\right] \times \left(\zeta_y - u_y\right) d\zeta_x d\zeta_y \quad (16)$$

The outgoing distributions at the boundaries are denoted by φ^+, ψ^+ and are expressed by the Maxwell purely diffuse reflection as (Pantazis, Valougeorgis, 2010)

$$\varphi^+ = \frac{n_w}{\pi\tau_w} \exp\left[-\left(\zeta_x^2 + \zeta_y^2\right) / \tau_w\right] \quad (17)$$

and

$$\psi^+ = \frac{n_w}{2\pi} \exp\left[-\left(\zeta_x^2 + \zeta_y^2\right) / \tau_w\right] \quad (18)$$

where τ_w is the dimensionless wall temperature and n_w is a parameter given in terms of the ingoing distributions satisfying the impermeability wall conditions.

The above set of integro-differential equations (4) and (5) coupled with the expressions (10-16) subject to boundary conditions (17) and (18) is numerically solved using the discrete velocity method (DVM). The implemented algorithm has been utilized to solve nonlinear flows and heat transfer problems with considerable success (Pantazis, Valougeorgis, 2010; Misdanitis et al., 2012; Pantazis at al., 2013). Thus, here only some limited information on the computational approach is provided.

The molecular velocities ζ_x and ζ_y are transformed to polar coordinates, according to $\zeta_x = \zeta\cos\theta$ and $\zeta_y = \zeta\sin\theta$. Then, the

continuum velocity spectrum (ζ,θ) is replaced by a set of discrete velocities (ζ_m,θ_n), with $m=1,2,...,M$ and $n=1,2,...,N$. The magnitudes ζ_m are taken to be the roots of the Legendre polynomial of order M accordingly mapped from $(-1,1)$ to $(0,+\infty)$, while the polar angles are $\theta_n=\pi(2n-1)/N$. In the physical space the flow domain is divided into $I\times J$ rectangular elements, with $i=1,2,...,I$ and $j=1,2,...,J$.

Equations (9) and (10) are discretized in the molecular space and the deduced set of partial differential equations is solved by a typical second-order finite volume scheme. The moments (10-16) are numerically integrated applying the trapezoidal rule in the polar angle θ and the Gauss-Legendre quadrature in the velocity magnitude ζ. The system of equations and their associated moments are solved in an iterative manner which is terminated when the convergence criteria

$$\varepsilon^{(k)}=\max_{i,j}\left\{\left|n_{i,j}^{(k)}-n_{i,j}^{(k-1)}\right|+\left|u_{xi,j}^{(k)}-u_{xi,j}^{(k-1)}\right|+\right.$$
$$\left.+\left|u_{yi,j}^{(k)}-u_{yi,j}^{(k-1)}\right|+\left|\tau_{i,j}^{(k)}-\tau_{i,j}^{(k-1)}\right|\right\}\le 10^{-13} \qquad (19)$$

is fulfilled. Here, k denotes the iteration index and $\varepsilon^{(k)}$ the error after k iterations. Upon convergence all conservation principles are accordingly preserved.

A well-known problem in this method is the propagation of boundary induced discontinuities, especially at high Knudsen numbers, known as ray effects. A simple procedure was used to cope with the discontinuous boundary conditions at the two corners of the bottom wall. Along a small length at the two ends of the bottom wall, equal to 5% of the total side length of the square cavity, the temperature is taken to have a linear variation between T_C and T_H. This way the ray effects were diminished.

3.2 DSMC formulation

The DSMC method is based on splitting the real process of particle motion in two consecutive steps: a) the collision between the particles which is modeled in a stochastic manner within the particles at a given cell, and b) the ballistic motion of the particles over a distance proportional to their velocities, which is purely deterministic.

Here, the space domain is discretized into 100x100 squared cells with size smaller than the mean free path, while the gas is represented by a discrete number of model particles. A total number of 10^6 model particles have been used and the time step was chosen to be about 1/3 of the cell traversal time $W/(n_C\upsilon_0)$, with n_C being the number of cells in the *x*-direction. The sampling of the macroscopic quantities starts once the steady state flow has been achieved and is carried out by volume based time averaging of the corresponding microscopic values of the particles at a given cell. These moments are accumulated over 10^5 time steps. This gives a sample size of approximately 10^7 particles per cell which is sufficiently large to reduce the statistical scatter of the macroscopic results.

The standard No Time Counter (NTC) scheme (Bird, 1994) together with the HS molecular interaction model, are used for computing the collision between the particles. The interaction of the gas molecules with the solid walls is assumed to be purely diffuse.

4. Results and discussion

The flow in the square cavity was simulated for $0.1\le Kn_0$ covering the transition and free molecular regimes and three temperature ratios $T_C/T_H=0.1$, 0.5 and 0.9. In all cases the hard sphere molecular interaction model ($\omega=1/2$) has been applied. Simulations have been conducted both by the deterministic and stochastic methods, and a very good agreement between corresponding results has been obtained.

In Figs. 2 and 3 the streamlines and the temperature contours for $T_C/T_H=0.1$ and $T_C/T_H=0.9$ are shown respectively for $Kn_0=0.1$, 1 and 10. At $Kn_0=0.1$ the largest part of the cavity is covered by the typical thermal creep type vortices I and vortices II are restricted near the side walls of the cavity. As the gas rarefaction is increased vortices II

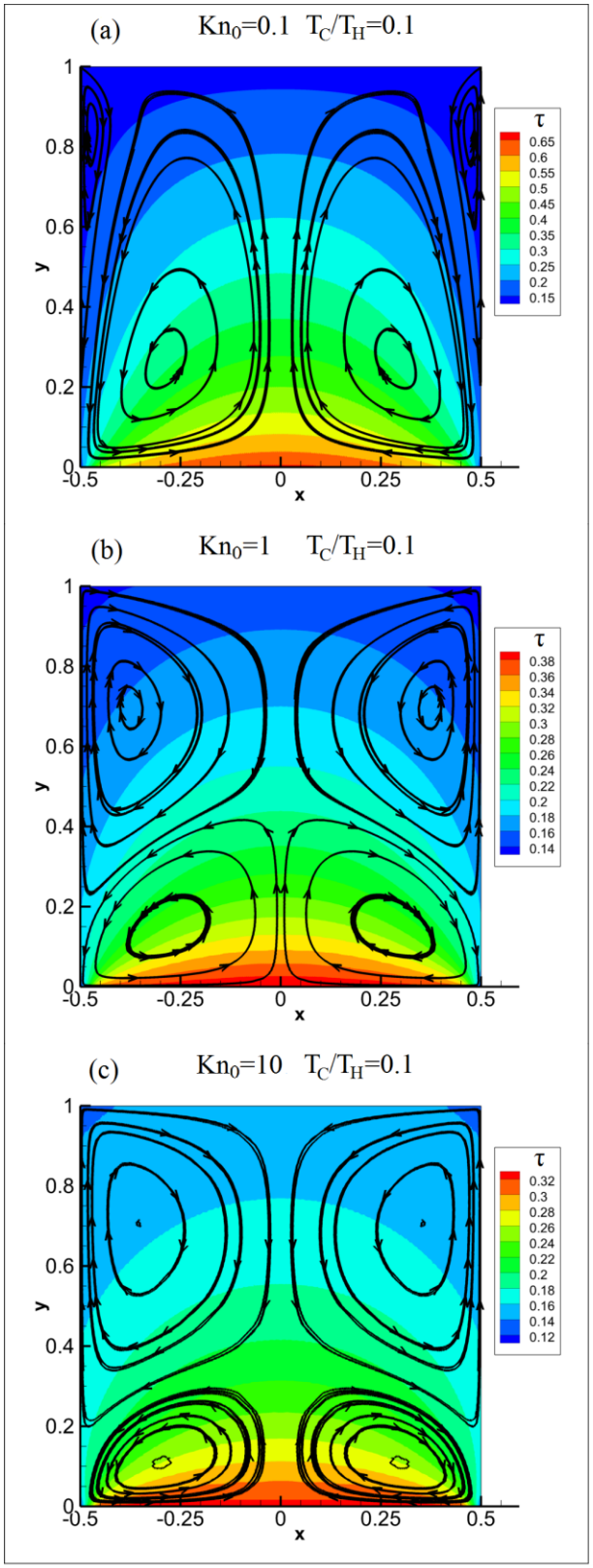

Fig. 2. Streamlines and temperature contours for $T_C / T_H = 0.1$ and various Knudsen numbers.

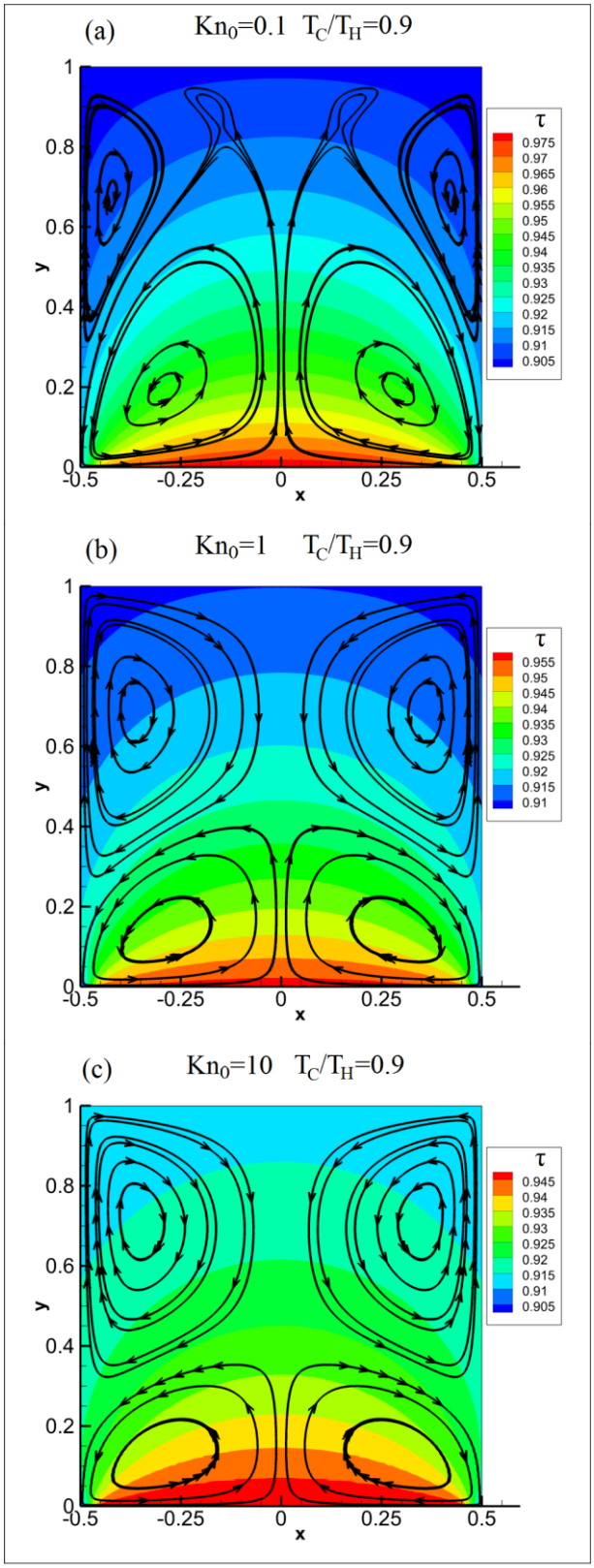

Fig. 3. Streamlines and temperature contours for $T_C / T_H = 0.9$ and various Knudsen numbers.

start to expand squeezing the vortices I towards the bottom part of the cavity. As it is seen at $Kn_0 = 1$, vortices II are already well developed covering large areas of the square cavity. The flow configuration is similar at $Kn_0 = 10$, with vortices I further squeezed towards the bottom of the cavity.

The above observations are valid for the temperature ratios of $T_C / T_H = 0.1$ and 0.9 corresponding to large and small temperature differences respectively. In all the cases tested, the vertical velocity near the lateral walls is positive for the biggest part of the wall, leading to the unexpected flow directed from hot-to-cold regions. Of course as the Knudsen number tends to infinity the gas velocity vanishes.

In Fig. 4 the u_y distribution along the lateral walls is shown. Due to symmetry these results correspond to $x = \mp 1/2$. Results are provided $T_C / T_H = 0.1, 0.5, 0.9$ corresponding to small, moderate and large temperature differences and in each case for $Kn_0 = 0.1, 1, 10$. The negative values of the velocity are related to the expected thermal creep flow from cold-to-hot, whereas the positive ones to the unexpected flow from hot-to-cold. We observe that even for small Knudsen numbers, and for all temperature ratios, in the biggest part of the wall the velocity is positive, leading to a mass flow rate from hot-to-cold. This phenomena has been explained when the flow is in the slip regime in (Rana et al., 2012). In the whole range of the Knudsen number it may be explained by splitting the flow into a ballistic and collision part. The exact physical explanation is provided in (Vargas et al, 2014).

Another quantity of practical interest is the average dimensionless heat flux q_{ave} departing from the bottom plate, which may be estimated by integrating the heat flux $q_y(x,0)$ over $x \in [-0.5, 0.5]$. This quantity is plotted in Fig. 5 in terms of Kn_0 for various temperature ratios T_C / T_H. The DSMC results are also presented for comparison purposes.

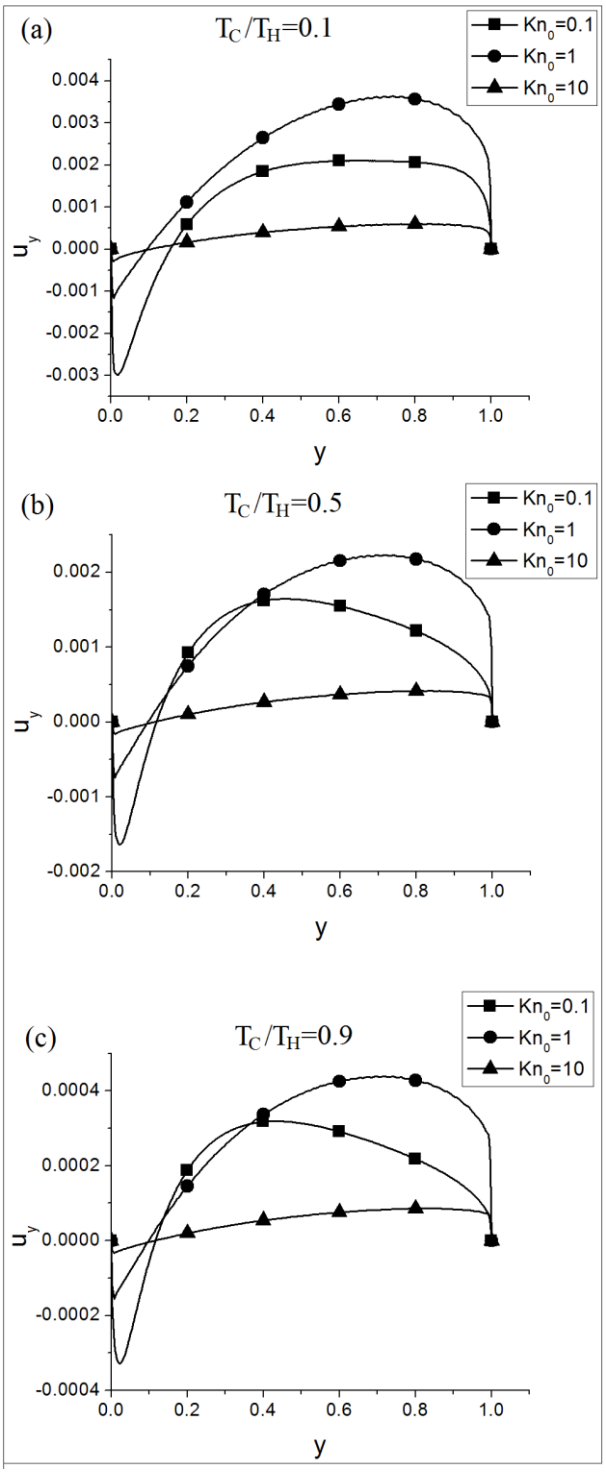

Fig. 4. Distribution of the tangential velocity u_y along the lateral walls of the square enclosure for various Knudsen numbers and temperature ratios.

As it is seen the agreement is very good in all cases. The average dimensionless heat flux increases as Kn_0 increases and tends to an asymptotic value as we approach the limiting case of $Kn_0 \to \infty$. A very interesting result is that for $Kn_0 > 0.5$, q_{ave} is not steadily increased as the temperature difference becomes greater. As it is seen it turns out that for $T_C / T_H = 0.5$ q_{ave} is larger than that for $T_C / T_H = 0.1$. This behavior has been captured by both modeling approaches.

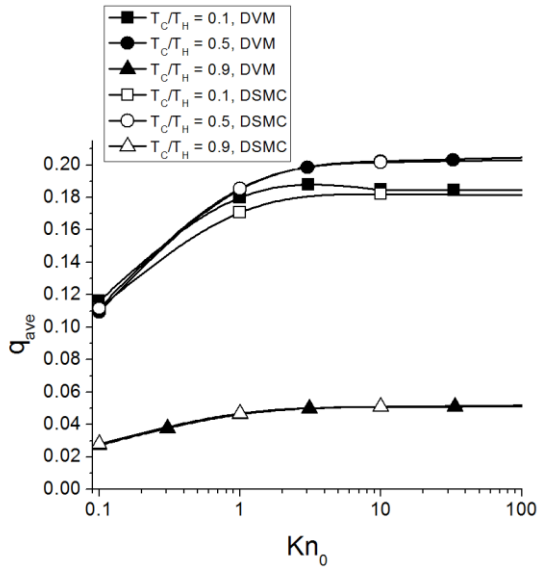

Fig. 5. Average heat flux q_{ave} departing from the bottom plate of a square enclosure in terms of the Knudsen number for various temperature ratios.

5. Concluding Remarks

A rarefied cavity flow with a single heated wall has been simulated. The two parameters characterizing the problem are the temperature ratio T_C / T_H and the reference Knudsen number Kn_0. Simulations have been conducted for $T_C / T_H = 0.1$, 0.5 and 0.9 and $Kn_0 = 0.1$, 1 and 10 using both the deterministic and DSMC methods.

A flow in the region of the lateral walls directed form hot-to-cold has been observed even for small temperature differences and small Knudsen numbers, confirming previous findings in similar set-ups (Rana et al., 2012). Another interesting finding was that the average heat flux departing from the bottom plate does not necessarily increase as the temperature difference increases. For relatively large Knudsen numbers, there is a maximum at $T_C / T_H = 0.5$.

Overall, it is believed that this work has both scientific and technological interest since such flows are very common in micro/nano-electromechanical systems.

Acknowledgments

This research obtained financial support from the European Community's Seventh Framework programme (FP7/2007-2013) under GA.215504.

References

Stone, H.A., Stroock, A.D., Ajdari, A., 2004. Engineering flows in small devices: microfluidics toward a lab-on-a-chip. Annual Reviews of Fluid Mechanics, 36, 381-411.

Yang, H.A., Wu, M.C., Fang. W.L., 2005. Localized induction heating solder bonding for wafer level MEMS packaging. Journal of Micromechanics and Microengineering, 15, 394-399.

Liu, H., Wang, M., Wang, J., Zhang, G., Liao, H., Huang, R., Zhang. X., 2007. Monte Carlo simulations of gas flow and heat transfer in vacuum packaged MEMS devices. Applied Thermal Engineering, 27, 323-329.

Sone, Y., Waniguchi, Y., Aoki, K., Takata. S., 1996. One-way flow of a rarefied gas induced in a channel with a periodic temperature distribution. Physics of Fluids, 8 (8), 2227-2235.

Alexeenko, A., Gimelshein, S., Muntz, E., Ketsdever. A., 2006. Kinetic modeling of temperature driven flows in short microchannels. International Journal of Thermal Sciences, 45, 1045-1051.

Ketsdever, A., Gimelshein, N., Gimelshein, S., Selden. N., 2012. Radiometric phenomena: From the 19th to the 21st century. Vacuum, 86, 1644-1662.

Vargas, M., Wüest, M., Stefanov. S., 2012. Monte Carlo analysis of thermal transpiration effects in capacitance diaphragm gauges with helicoidal baffle system. Journal of Physics: Conference 362, 012013.

Masters, N., D., Ye., W., 2007. Octant flux splitting information preservation DSMC method for thermally driven flows. Journal of Computational Physics, 226, 2044-2062.

Rana, A., Torrilhon, M., Struchtrup. H., 2012. Heat transfer in micro devices packaged in partial vacuum. Journal of Physics: Conference Series, 362, 012034.

Huang, J., C., Xu, K., Yu. P., 2013. A unified gas-kinetic scheme for continuum and rarefied flows III: Microflow simulations. Communications in Computational Physics, 14 (5), 1147-1173.

Cai. C., 2008. Heat transfer in vacuum packaged microelectromechanical system devices. Physics of Fluids, 20, 017103.

Sone. Y., 2009. Comment on "Heat transfer in vacuum packaged microelectromechanical system devices" [Phys. Fluids 20, 017103 (2008)], Physics of Fluids, 21, 119101.

Naris, S., Valougeorgis, D., Gas flow in a grooved channel due to pressure and temperature gradients. in Proceedings ICNMMM2006-96225 June 19-21, 2006 (ASME, New York, 2006)

Struchtrup, H., Taheri. P., 2011. Macroscopic transport models for rarefied gas flows: A brief review. IMA Journal of Applied Mathematics, 76 (5) 672-697.

Sone. Y., 2002. Kinetic Theory and Fluid Dynamics, Birkhäuser, Boston.

Bird. G., A., 1994. Molecular Gas Dynamics and the Direct Simulation of Gas Flows. Clarendon, Oxford.

Shakhov. E., M., 1968. Generalization of the Krook kinetic relaxation equation, Fluid Dynamics, 3(5), 142-145.

Sharipov, F., Seleznev. V., 1998. Data on Internal Rarefied Gas Flows. Journal of Physical and Chemical Reference Data, 27, 657–706.

Cercignani. C., 1988. The Boltzmann equation and its Applications, Springer, New York.

Pantazis, S., Valougeorgis. D., 2010. Non-linear heat transfer through rarefied gases between coaxial cylindrical surfaces at different temperatures. European Journal of Mechanics B/Fluids, 29, 494-509.

Misdanitis, S., Pantazis, S., Valougeorgis. D., 2012. Pressure driven rarefied gas flow through a slit and an orifice. Vacuum, 86, 1701-1708.

Pantazis, S., Naris, S., Tantos, C., Valougeorgis, D., Andre, J., Millet, F., Perin. J., P., 2013. Nonlinear vacuum gas flow through a short tube due to pressure and temperature gradients. Fusion Engineering and Design, 88, 2384-2387.

Vargas, M., Tatsios, G., Valougeorgis, D., Stefanov. S., 2014. Rarefied gas flow in a rectangular enclosure induced by non-isothermal walls. Physics of Fluids, 26, 057101